ChemComm

Accepted Manuscript

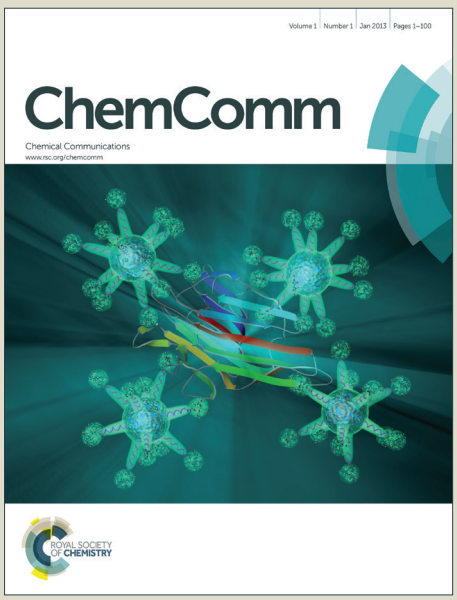

This is an *Accepted Manuscript*, which has been through the Royal Society of Chemistry peer review process and has been accepted for publication.

Accepted Manuscripts are published online shortly after acceptance, before technical editing, formatting and proof reading. Using this free service, authors can make their results available to the community, in citable form, before we publish the edited article. We will replace this *Accepted Manuscript* with the edited and formatted *Advance Article* as soon as it is available.

You can find more information about *Accepted Manuscripts* in the Information for Authors.

Please note that technical editing may introduce minor changes to the text and/or graphics, which may alter content. The journal's standard Terms & Conditions and the Ethical guidelines still apply. In no event shall the Royal Society of Chemistry be held responsible for any errors or omissions in this *Accepted Manuscript* or any consequences arising from the use of any information it contains.

ROYAL SOCIETY OF CHEMISTRY

www.rsc.org/chemcomm

Journal Name

RSCPublishing

COMMUNICATION

Probing the kinetics of lipid membrane formation and the interaction of a nontoxic and a toxic amyloid with plasmon waveguide resonance

Cite this: DOI: 10.1039/x0xx00000x

Received 00th January 2012,
Accepted 00th January 2012

DOI: 10.1039/x0xx00000x

www.rsc.org/

E. Harté,[a] N. Maalouli, [b] A. Shalabney, [c] E. Texier, [d] K. Berthelot, [e] S. Lecomte and [a] I. D. Alves [a*]

The kinetics of formation of solid-supported lipid model membranes was investigated using a home-made plasmon waveguide resonance (PWR) sensor possessing enhanced properties relative to classic surface plasmon resonance sensors. Additionally, kinetics of interaction of two amyloid peptides with zwitterionic and anionic membranes and effect on lipid organization was followed.

Surface plasmon resonance (SPR) has been widely used to monitor a large range of molecular interactions directly and in real time. Plasmon-waveguide resonance (PWR) spectroscopy combined with techniques for forming solid-supported proteolipid membranes allows kinetic, thermodynamic and structural characterization of anisotropic thin films.[1] This technique possesses several important advantages that make it especially well suited for studies of lipid membranes: 1) spectral analysis yields a complete characterization of thin film optical parameters, i.e., refractive index *n* and extinction coefficient *k* as well as the film thickness *t*. Contrarily to SPR, PWR measurements can be performed with light polarized both parallel (*p*-) and perpendicular (*s*-) to the incident plane, for large incident angles (which are used here), in *p*-polarization light the electric vector becomes perpendicular to the film plane and in *s*-polarized parallel to the film plane. This allows the characterization of both birefringent and dichroic systems. 2) The methodology involves the use of evanescent waves (surface-bound electromagnetic waves) that are generated under resonance conditions providing much narrower linewidths than those of conventional SPR and an exceptionally high sensitivity. 3) The silica surface covering the plasmon generating media (metal film) protects it mechanically and chemically against corrosion increasing the sensor lifetime. The technique has been used to follow activation and signalling of G-protein coupled receptors (GPCRs)[2, 3, 4, 5] and the interaction of membranotropic molecules with lipid membranes.[6, 7] A home-made PWR instrument was recently built in our laboratory possessing enhanced properties relative to the one previously reported in the literature.[1] Namely, this instrument allows faster data acquisition with kinetics in the msec scale (for single angle measurements) and the possibility to obtain resonances simultaneously (within the same angular scan measurement) with both *p*- (transverse magnetic, TM) and *s*- (transverse electric, TE) polarized light. This is accomplished by appropriately choosing the polarization angle of the incident light beam to possess both electric fields (Figure 1). Usually a value of 45° would ensure that the incident light photons would be equally distributed between the *p*- and *s-pol*s. In our case we have used an angle of 51° to favour the *s*-pol relative to the *p*-pol and to improve the S/N ratio of the *s*-pol resonance, which inherently is less deep. Following simultaneously both polarizations is especially advantageous to study oriented anisotropic molecules such as lipid membranes.

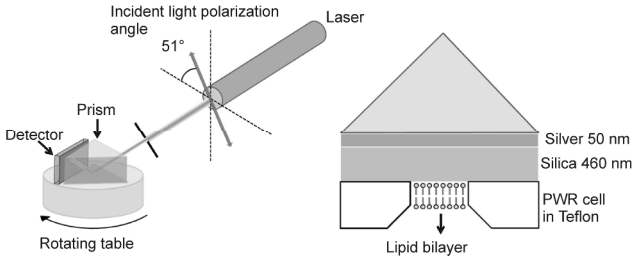

Figure 1. PWR setup. On the left the optical and mechanical components, the incident polarized light beam (a continuous wave laser He-Ne laser at 632.8 nm) is at 51° and the rotating table allows steps of 1 millidegree. On the right is a detailed view of the prism and the PWR cell sample with the lipid bilayer.

To evaluate the high potentiality of our instrument we investigated the process of formation of a lipid bilayer and the interaction of amyloid peptides. Many *in vitro* studies have pointed out the key role of the interaction between amyloids and lipid membranes and their potential involvement in amyloid toxicity.[8] In the last few years we developed in the yeast *Saccharomyces cerevisiae* a model of amyloid toxicity based on toxic mutants of the HET-s prion of *Podospora anserina*.[9, 10] This amyloid peptide fulfils in the fungus the beneficial function of heterokaryon incompatibility which leads to a process of localized cell death to avoid the fusion of incompatible hyphae.[11] The amyloid part of this prion is the domain HET-s$_{(218-289)}$ [wild-type (WT)], which is one of the most structurally studied amyloid with a fiber in a characteristic parallel β-sheet solenoid structure.[12] This domain is not toxic when expressed in the yeast *S. cerevisiae*, and we previously generated a toxic (called the M8) mutant by random mutagenesis.[9] This mutant

ChemComm Accepted Manuscript

possesses 10 mutations and greatly differs from the WT domain both biochemically and structurally. M8 is organized in amyloid nanofibers with a cross-beta core of antiparallel β-sheet and presents particular oligomeric intermediates.[10 13] Screening for yeast genes involved in M8 toxicity, we demonstrated that M8 toxicity was probably mediated through lipid membranes by strongly interfering with vesicular trafficking in the yeast cells.[14] In previous studies we established that M8 binding to anionic lipids promotes its aggregation and formation of microdomains ("amyloid rafts") accompanied by significant membrane leakage. The WT peptide only binds to the membrane organizing itself in the form of isolated fibers with no aggregation or membrane disruption.[15 16] Using PWR the kinetics of bilayer formation and interaction of two amyloid peptides: the non-toxic wild-type (WT) form and the toxic mutant (M8) were investigated. So far no information regarding the kinetic rates for the interaction of these and other amyloid peptides with membranes has been reported in the literature. One of the reasons relates to the highly dynamic behaviour of these peptides in terms of its aggregation upon often small changes in concentration, temperature, pH and lipid contact.

Herein, we have followed by PWR the kinetics of formation of a solid-supported lipid membrane prepared by the same procedure used by Mueler and Rudin to prepare black lipid membranes (BLM) .[17] Briefly, the method consists in spreading about 2.2 μL of a lipid solution (in our case DOPC and DOPG, 10 mg/mL in squalene/BuOH/MeOH 0.05:9.5:0.5, v/v) across a small orifice (4 mm) in a Teflon block that constitutes the cell sample compartment (Figure 1). The hydrophilic SiO_2 surface is covered with a thin layer of water of condensation [18 19] and attracts the polar groups of the lipid molecules with the hydrocarbon chains oriented toward the bulk lipid phase, which induces an initial orientation of the lipid molecules. The next step involves addition of aqueous buffer to the sample compartment of the PWR cell, which results in formation of an annular plateau-Gibbs border of lipid solution that anchors the membrane to the Teflon spacer. This border allows membrane flexibility wherein the bilayer can deform and lipid molecules can become displaced or recruited upon insertion or conformational changes of proteins or peptide "detergent effect" in the membrane. One should point that the solid-supported membrane formed by this method contains residual amounts of organic solvents (specially squalene) and thus differs from membranes formed by vesicle fusion. Kinetics of formation of model membranes is rather limited in the literature with no rate constants being provided as it is the case in dual polarization interferometry study.[20] Right after the addition of buffer to the lipid solution for membrane formation, resonances were acquired with both *p*- and *s*-polarized light to follow the membrane formation procedure. An immediate increase in the resonance angle position relative to the buffer spectra was observed for both polarizations indicating an increase in the mass of the system relative to the buffer. Then, the resonance in *p-pol* kept on shifting to higher angles with time until equilibrium was reached. With *s*-polarized light the opposite was observed with a decrease in the resonance angle position. Overall the formation of the membrane resulted in final resonance shifts positive for both polarizations and higher in *p*-pol than with *s*-pol (185 ± 37 *vs* 88 ± 26 mdeg, Figure 2, Panel A, B, C). This is expected as the refractive index of lipids is superior to that of the buffer that it replaces resulting in resonances at higher angles. Moreover, shifts in the *p*-pol were higher than in *s*-pol indicating that the refractive index for *p*-pol (n_p) is higher than that of the *s*-pol (n_s) with a Δs/Δp of about 0.5 (Figure 2D). This is

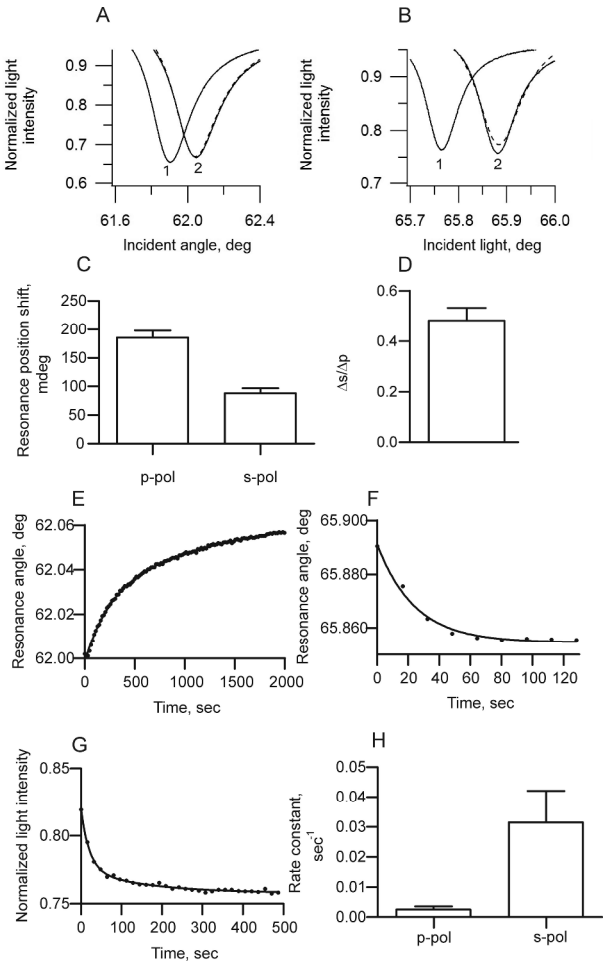

Figure 2. Formation of planar lipid bilayer. PWR spectra of buffer (1) and after formation and stabilization of a DOPG bilayer (2) obtained with *p*- (A) and *s*-polarized (B) light. In the bilayer spectra (2) the theoretical fits to the data are presented in dashed lines and the optical parameters are given in the text. The resonance positions shifts observed with *p*- and *s*-polarized light upon bilayer formation (both DOPG and DOPC) and stabilization as well as the ratio between the two (Δs/ Δp) are presented in Figure C and D, respectively for 10 independent experiments. The kinetics of bilayer formation (DOPG) in terms of the changes in the resonance angle position for *p*- and *s*-polarized light and spectral depth obtained with *s*-pol are presented in E, F and G, respectively. The rate constants k obtained for the changes in the resonance minimum position for *p*- and *s*-polarized from 7 experiments (both DOPC and DOPG) are presented in Figure H and were 0.003 ± 0.001 sec^{-1} for *p*-pol and 0.03 ± 0.01 sec^{-1} for *s*-pol. The measurements were conducted at 23°C.

the proof that the membrane is properly oriented with the longer axis perpendicular to the prism surface (parallel to the *p*-pol) .[1 21 22]

Fits of experimental spectra to theoretical ones based on Maxwell's equations were performed using the 4x4 propagation matrices approach.[23] The multi-layers system namely silver, silica, lipid membrane, and the protein, was assumed to be embedded between two semi-infinite, homogenous, and isotropic media represented by the prism coupler and the buffer.

Since the optical properties of each of these layers are orientation dependent, the anisotropy was described using the dielectric tensor for every slab. Assuming that the incidence beam is linearly polarized, the experimental data were fitted by

ChemComm Accepted Manuscript

This journal is © The Royal Society of Chemistry 2012

weighting both the theoretical *p* and *s* polarization reflectivities. A full description of the theoretical model that was used in this study can be found in the appendix of reference.[23] From the fits presented (dashed lines in Figure 2A and B) a n_p of 1.62 and n_s of 1.45 were obtained, values that agree with those reported previously by PWR and other methods. [1 24 25 26] A thickness (*t*) of 6 ± 0.5 nm was obtained for the bilayer, a value slightly above values determined by other methods due to the highly ordered nature of this membrane resulting from the presence of hydrocarbon. These optical parameters confirm the formation of one properly oriented membrane. The kinetics of the changes in the resonance position and in normalized light intensity (spectral depth) for both polarizations were obtained by fitting the data by a one-phase exponential association (Graph Pad Prism) (Figure 2 E, F, G, H). One should note kinetics data acquisition started only after filling the cell sample with buffer following the addition of lipid solution. Rate constants for changes in the resonance position were of 0.003 ± 0.001 sec^{-1} for the *p-pol* and 0.03 ± 0.01 sec^{-1} for *s-pol* (Figure 2H). Spectral depth, a parameter both correlated with the bilayer thickness and refractive index did not change for *p*-pol and increased for the *s*-pol, indicating membrane thinning over time. The rate of spectral depth changes observed with the *s*-pol was 0.03 sec^{-1}, a value similar to the rate of resonance minimum position shift (Figure 2). The bilayer thickness represents an average molecular length perpendicular to the plane of the film that is independent of light polarization.

The data is interpreted as follows: right after painting the membrane across the Teflon orifice and filling the PWR cell sample with buffer, the lipid headgroups are already oriented towards the silica surface in the prism. In *s-pol* in the first few spectra one can see additional fringes at higher angles of resonance (data not shown) that correspond to organic solvent (butanol and methanol) still remaining in the membrane. With time they disappear and a single symmetric resonance is seen. The resonance minimum position increases in *p*-pol and decreases in *s*-pol with time, this is correlated with an increase in the refractive index in *p*-pol and a decrease in *s*-pol, that is an overall increase in the anisotropy of the bilayer, this is interpreted as change in lipid tilting with time and increased lipid ordering accompanied by changes in membrane thickness. Membrane formation reaches equilibrium in less than 30 min. The kinetics of bilayer formation was the same for zwitterionic (DOPC) and anionic lipids (DOPG) lipids, the hydrophobic interactions leading the process. This is as far as we know the first time rate constants are provided in kinetic studies of model membrane formation.

The interaction of the non-toxic (WT) and toxic (M8) amyloid peptides with DOPC and DOPG membranes were investigated by PWR. Protein preparation and purification can be found in ref 11. While in all scenarios peptide addition leads to increase in the resonance angle position, showing that the peptides bound to the membrane (leading to increase in the refractive index and mass of the proteolipid system), the magnitude of those shifts, the kinetics of the interaction and their effect on the lipid membrane organization was quite different for the two lipids and the two peptides. The larger spectral shifts were observed for the peptide interactions with DOPG (Table 1, Figure 3, Figure 1 in SI), and in the case of M8 the spectral shifts were accompanied by a split in the *s*-pol resonance (Table 1, Figure 3). Larger spectral shifts indicate that more peptide is present on the membrane surface with larger membrane reorganization occurring to accommodate the peptide.

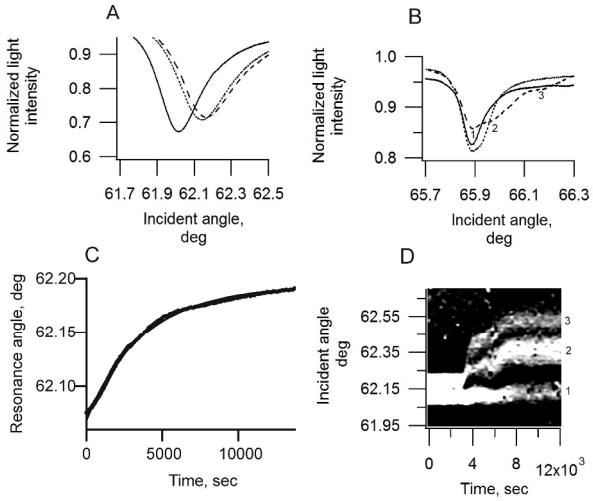

Figure 3. Interaction of amyloid peptide M8 with a DOPG bilayer. PWR spectra of a DOPG bilayer alone (solid line) and after addition of peptide after 15 min (small dashed) and at equilibrium (large dashed) for *p*- (A) and *s*-pol (B) light. Domains in the membrane are represented as 1, 2 and 3 (details are in the text). Kinetics of M8 interaction with DOPG obtained with *p*-pol (C) (rate constants are presented in Table 2). The image D represents the second derivative of the intensity of the s-pol resonances (shown in B) as a function of the incident angle. The measurements were conducted at 23°C.

Table 1. Magnitude of spectral shifts (millidegree, mdeg) upon amyloid interaction with the lipid membrane.

Amyloid	WT		M8	
Polarization	*p*	*s*	*p*	*s*
DOPC	10	20	52	55
DOPG	48	76	61	[a]63, 160

[a] estimated values for the two resonances observed.

The appearance of additional resonances in the *s-pol* can be attributed to a heterogeneity in the peptide assembling in the membrane with the presence of regions (domains) possessing different mass and organization. The appearance of additional resonances in this polarization have been observed for membranes containing mixtures of lipid ordered and disordered domains and have been attributed to microdomain formation.[8 27] Taking into account the capability of amyloid peptides to oligomerize and to form fibers and platelets,[8, 16] the multiple resonances seen can correspond to those different oligomeric states of the peptides. Overall the larger spectral shifts observed for both peptides in the case of DOPG indicate that electrostatic interactions with the membrane promote larger peptide accumulation, this data agrees with previously reported studies from our laboratory. [15 27]

Spectral fitting indicates that both M8 and WT increase the DOPC membrane thickness by 2.7 ± 0.2 nm. In the case of DOPG, the membrane thickness increases by 3 ± 0.2 nm for the WT. For M8 three different domains in the membrane can be distinguished when analyzing the *s*-pol data corresponding to different peptide organizations (Figure 3B): the larger fringe placed at lower incident angle (labelled 1 in Fig 3B) corresponds to 60% of the area of the membrane where no increase in thickness is observed (domain without peptide adsorbed); the second fringe placed at higher incident angles (labelled 2 in Fig. 3B) corresponds to 25% of membrane area and to a region with peptide possessing an increased

ChemComm Accepted Manuscript

thickness of 6 ± 0.5 nm relative to the membrane alone; the fringe located at larger incident angle (less deep one, labelled 3 in Fig. 3B) covers 15% of the membrane and corresponds to an area of the membrane where the peptide is highly present and aggregated in large domains with increased thickness of 10 ± 0.8 nm relative to the bare membrane. These calculations correlate very well with those observed by image analysis of the second derivative of the intensity as a function of the incident angle representing the kinetics evolution obtained with s-pol following M8 addition to the membrane (Fig. 3C) After M8 injection at ~ 2.5 X 10^3 sec three domains are observed: domain 1 that represents membrane not covered by peptide (the angle remains the same as before injection); a second domain is formed with a higher resonance minima that remained for about 190 sec before it split into two domains that are shifted by +24 mdeg and +38 mdeg relative to the bilayer (2 and 3, respectively) and correspond to regions of the membrane where the peptide accumulates. The relative shifts of the two domains correlate well with the thickness increases provided of 6 and 10 nm for domains 2 and 3, respectively.

As for the kinetics of M8 and WT interaction with the membranes there are no particular differences between the two peptides (Table 2). When comparing the two lipid systems, peptide interaction and membrane reorganization is slower with DOPG probably due to the fact that more peptide is binding and more lipid and peptide organization is taking place after the first contact.

Table 2. Kinetics of amyloid interaction with the lipid membrane. Rate constants have been obtained by a one phase exponential association and are expressed in sec^{-1}.

Amyloid	WT		M8	
Polarization	*p*	*s*	*p*	*s*
DOPC	2 x 10^{-3} ± 10^{-4}	6 x 10^{-4} ± 3 10^{-5}	2 x 10^{-3} ± 4 10^{-5}	6 x 10^{-3} ± 1 10^{-4}
DOPG	5 x 10^{-4} ± 1 10^{-5}	3 x 10^{-3} ± 8 10^{-5}	3 x 10^{-4} ± 1 10^{-6}	4 x 10^{-4} ± 7 10^{-6}

Overall the data also indicates that independently from the amount of peptide bound to the membrane, there are always membrane areas that are not covered by peptide, meaning that the peptide preferentially interacts with the membrane already coated with peptide. The work described here shows that PWR with the capacity to follow changes in oriented anisotropic films and with the enhanced data acquisition rate is a useful method to follow the kinetics of lipid membrane formation and molecular orientation as well as the interaction of proteins/peptides and domain formation in membranes.

Notes and references

[a]CBMN, UMR 5248 CNRS, Université de Bordeaux, Allée Geoffroy St. Hilaire, 33600 Pessac (France), Fax: (+33) 5-40002220 ; E-mail: i.alves@cbmn.u-bordeaux.fr

[b]Departamento de Química de los Materiales, Universidad de Santiago de Chile, Avenida Libertador Bernardo O'Higgins nº 3363 (Chile).

[c]ISIS, Université de Strasbourg, 8 allée Gaspard Monge, 67083 Strasbourg (France)

[d]CRPP, Université de Bordeaux, Avenue Schweitzer, 33600 Pessac (France)

[e] LCPO UMR 5629 CNRS, Université de Bordeaux, 16 av.Pey-Berland, 33600 Pessac (France)

Electronic Supplementary Information (ESI) available. See DOI: 10.1039/c000000x/

1 Z. Salamon, H. A. Macleod, G. Tollin, *Biophys. J.,* 1997, **73**, 2791-2797.

2 I. D. Alves, Z. Salamon, E. Varga, H. I. Yamamura, G. Tollin, V. J. Hruby, *J. Biol. Chem.,* 2003, **278**, 48890-48897.

3 I. D. Alves, G. F. Salgado, Z. Salamon, M. F. Brown, G. Tollin, V. J. Hruby, *Biophys. J.,* 2005, **88**, 198-210.

4 I. D. Alves, Z. Salamon, V. J. Hruby, G. Tollin, *Biochemistry,* 2005, **44**, 9168-9178.

5 I. D. Alves, D. Delaroche, B. Mouillac, Z. Salamon, G. Tollin, V. J. Hruby, S. Lavielle, S. Sagan, *Biochemistry,* 2006, **45**, 5309-5318.

6 I. D. Alves, I. Correia, C. Y. Jiao, E. Sachon, S. Sagan, S. Lavielle, G. Tollin, G. Chassaing, *J. Pept. Science,* 2009, **15**, 200-209.

7 I. D. Alves, C. Bechara, A. Walrant, Y. Zaltsman, C. Y. Jiao, S. Sagan, *PloS one,* 2011, **6**, e24096.

8 G. F. Salgado, A. Vogel, R. Marquant, S. E. Feller, S. Bouaziz, I. D. Alves, *J. Med. Chem.,* 2009, **52**, 7157-7162.

9 K. Berthelot, C. Cullin, S. Lecomte, *Biochimie,* 2013, **95**, 12-19.

10 J. Couthouis, K. Rebora, F. Immel, K. Berthelot, M. Castroviejo, C. Cullin, *PloS one,* 2009, **4**, e4539.

11 K. Berthelot, F. Immel, J. Gean, S. Lecomte, R. Oda, B. Kauffmann, C. Cullin, *FASEB J.,* 2009, **23**, 2254-2263.

12 V. Coustou, C. Deleu, S. Saupe, J. Begueret, *Proc. Nat. Acad. Sci. USA,* 1997, **94**, 9773-9778.

13 C. Wasmer, A. Lange, H. Van Melckebeke, A. B. Siemer, R. Riek, B. H. Meier, *Science,* 2008, **319**, 1523-1526.

14 K. Berthelot, S. Lecomte, J. Gean, F. Immel, C. Cullin, *Biophys. J.,* 2010, ***99***, 1239-1246.

15 J. Couthouis, C. Marchal, F. D'Angelo, K. Berthelot, C. Cullin, *Prion* 2010, **4**, 283-291.

16 H. P. Ta, K. Berthelot, B. Coulary-Salin, S. Castano, B. Desbat, P. Bonnafous, O. Lambert, I. Alves, C. Cullin, S. Lecomte, *Biochim. Biophys. Acta,* 2012, **1818**, 2325-2334.

17 P. Mueller, D. O. Rudin, *J. Theor. Biol.,* 1968, **18**, 222-258.

18 M. L. Gee, T. W. Healy, L. R. White, *J. Col. Interf. Sci.,* 1990, **140**, 450-465.

19 P. Silberzan, L. Léger, D. Ausserré, J. J. Benattar, *Langmuir,* 1991, **7**, 1647-1651.

20 A. Mashaghi, M. Swann, J. Popplewell, M. Textor, E. Reimhult, *Anal. Chem.,* 2008, **80**, 3666-3676.

21 G. Tollin, Z; Salamon, V. J. Hruby, *Trends Pharmacol. Sci.,* 2003, 24, 655-659.

22 Z. Salamon, G. Tollin, *Biophys. J.* 2004, **86**, 2508-2516.

23 A. Shalabney, C. Khare, B. Rauschenbach, I. Abdulhalim, *Sensors and Actuators, B: Chemical,* 2011, **159**, 201-212.

24 Z. Salamon, S. Devanathan, I. D. Alves, G. Tollin, *J. Biol. Chem.* 2005, **280**, 11175-11184.

25 E. Reimhult, M. Zach, F. Hook, B. Kasemo, *Langmuir,* 2006, **22**, 3313-3319.

26 Z. Salamon, Y. Wang, J. L. Soulages, M. F. Brown, G. Tollin, *Biophys. J.,* 1996, **71**, 283-294.

27 H. P. Ta, K. Berthelot, B. Coulary-Salin, B. Desbat, J. Gean, L. Servant, C. Cullin, S. Lecomte, *Langmuir,* 2011, **27**, 4797-4807.

ChemComm Accepted Manuscript

 This journal is © The Royal Society of Chemistry 2012